ACS Chemical Neuroscience

pubs.acs.org/chemneuro
Letter

Selection of DNA Aptamers That Promote Neurite Outgrowth in Human iPSC-Derived Sensory Neuron Organoid Cultures

Brandon Wilbanks,[#] Jenelle Rolli,[#] Keenan Pearson, Sybil C. L. Hrstka, Ronald F. Hrstka, Arthur E. Warrington, Nathan P. Staff, and L. James Maher III*

Cite This: *ACS Chem. Neurosci.* 2025, 16, 1258−1263
Read Online

ABSTRACT: Sensory neurons in the dorsal root ganglia transmit sensory signals from the periphery to the central nervous system. Induced pluripotent stem cell derived models of sensory neurons and dorsal root ganglia are among the most advanced available tools for the study of sensory neuron activity and development in human genetic backgrounds. However, few available reagents modify sensory neuron growth with disease or other model-relevant outcomes. Small molecules, peptides, or oligonucleotides that predictably alter sensory neuron behavior in these contexts would be valuable tools with potentially wide-ranging application. Here we describe the selection and characterization of DNA aptamers that specifically interact with human sensory neurons. Several selected aptamers increase neurite outgrowth from sensory neuron organoid cultures after single-dose treatments.

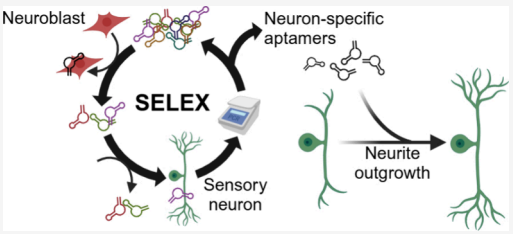

KEYWORDS: *DNA aptamer, neuron organoid culture, neurite outgrowth*

Sensory neurons are responsible for reception and signal transduction of pain, pressure, temperature, and other sensations.[1] Disorders of sensory neuron function, which often present as polyneuropathy, can arise from diabetes, autoimmune disease, hereditary conditions, and neurotoxic chemotherapeutic treatment.[2−6] Localized, aberrant neuron sprouting has also been implicated in chronic pain from arthritis, skeletal tumor metastases, and anticancer agents.[7−9] Modulators of sensory neuron behavior, whether they promote or inhibit neurite outgrowth, are therefore desirable as potential therapeutics. Reagents that alter neurite properties for potential therapy are most accurately studied in cultures of human cells. Such studies are facilitated by the exploitation of fibroblast-derived induced pluripotent stem cells (iPSCs) for the differentiation of neuron models. Commonly studied derivatives include iPSC-derived mature sensory neurons (iSNs) and dorsal root ganglion organoids (DRGOs), which model clusters of sensory neuron bodies coordinating communication between the peripheral and central nervous systems.

Human IgM antibodies eliciting biological responses in neuron models have been previously identified by screening natural human serum antibody libraries for binding affinity to cells of interest. One recombinant antibody identified using this approach, IgM22, has been shown to elicit neuroregenerative responses in a murine model of multiple sclerosis.[10] Other selected antibodies from this method, such as IgM12 and IgM42, have been found to promote neurite outgrowth in cell culture.[11] Inspired by these results, we have been using cell culture selections from vast libraries containing $\sim 10^{14}$ unmodified 80-mers to identify unmodified DNA aptamers that bind living cultured cells of interest and then screening among cell type-specific binders for those that alter biological activity.

Aptamers are single-stranded RNA or DNA molecules that tightly bind to purified target ligands or cells based on their interactions in 3-dimensional space. Chemically unmodified DNA aptamers are advantageous when compared to biologically active antibodies such as IgM12, -22, and -42 because of their low cost and exceptional degree of batch-to-batch reproducibility through chemical synthesis. In order to identify such high affinity and cell-type-specific reagents, we performed 15 rounds of selection from vast combinatorial oligonucleotide libraries in an effort to identify cell-binding DNA aptamers potentially relevant to disease modeling or therapeutics. Here we report the characterization of several resulting DNA aptamers that bind mature iPSC-derived iSNs but not neural precursor cells. Three of these aptamers enhance DRGO neurite outgrowth after a single treatment in the culture. To our knowledge, these are the first synthetic molecules demonstrated to elicit neurite outgrowth in human DRGO models. Other reports have identified aptamers specific to neurite targets on human model cell lines, but notably, these

Received: March 5, 2025
Revised: March 14, 2025
Accepted: March 14, 2025
Published: March 18, 2025

https://doi.org/10.1021/acschemneuro.5c00162
ACS Chem. Neurosci. 2025, 16, 1258−1263

have not been described to promote neurite outgrowth in the presence of standard growth media.[12,13]

In order to identify iSN-specific DNA aptamers, we applied 15 rounds of in vitro cell culture selection using an 80-nt DNA library containing 40 random positions. We used adherent SH-SY5Y neuroblastoma cells as negative selection targets (Figure 1A; Supplemental Figures S1A,B; Supplemental Table S1).

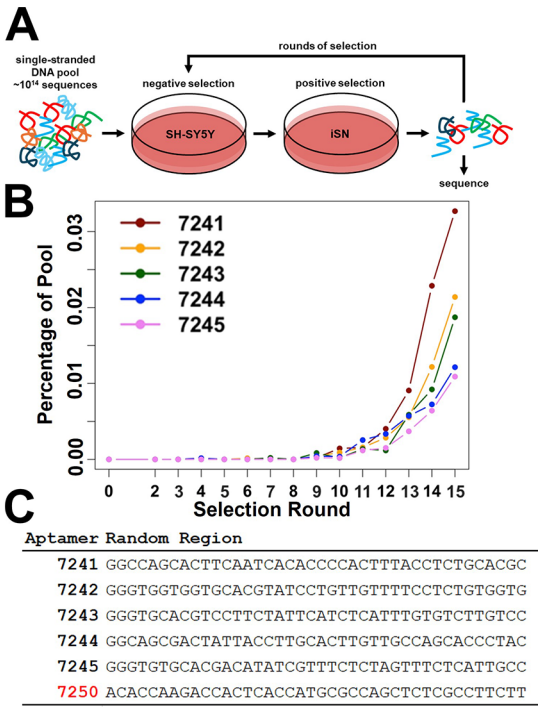

Figure 1. Selection and characterization of DNA aptamers targeting iSNs. (A) Schematic illustration of the selection approach used in this work. Aptamers were subjected to negative selection against immature neuroblast model SH-SY5Y cells. (B) Deep sequencing demonstrates enrichment of candidate aptamers used in this study over 15 rounds of selection. (C) Random regions (40 nt) and serial identification numbers of selected DNA aptamers. Negative control oligonucleotide 7250 is a shuffled version of aptamer 7241 retaining the same nucleotide composition.

SH-SH5Y cells are derived from immature neuroblasts, which we reasoned would be an appropriate negative selection target to isolate aptamer binding preferentially to fully differentiated cells in iSN cultures.[14] The targeted iSNs were generated from fibroblasts representing three healthy human donors in order to select aptamers with generic rather than donor-specific, properties. Donor fibroblast sources alternated round-to-round, while the negative selection SH-SH5Y cells remained unchanged.

We observed enrichment of five aptamer candidates, numbered as 7241−7245 (Figure 1B), which were then tested for binding to three cell types of interest: selection-targeted iSNs, negative selection SH-SH5Y cells, and mature differentiated SH-SY5Y cells. Candidate aptamers were synthesized as 3′ biotin conjugates to enable detection by fluorescent streptavidin and incubated with cells of interest at a concentration of 200 nM in wash buffer for 30 min at 37 °C. We first challenged aptamer candidates with binding to target iSNs and observed that all five aptamers bound iSNs more strongly than negative control molecule 7250, a sequence-shuffled version of 7241 with the same nucleotide composition (Figure 1C). This result was validated by quantitative PCR-based measurement of molecules bound to target iSN cells under the same conditions (Supplemental Figure S2). We next tested each aptamer for binding to differentiated SH-SY5Y cells, a model known to express more mature neuronal markers than the undifferentiated SH-SH5Y cells used for negative selections.[15] Four of the five selected aptamers bound to differentiated SH-SY5Y cells. Importantly, no selected aptamers bound to the immature undifferentiated SH-SY5Y cells that had been used for negative selection (Figure 2), suggesting that the aptamers recognize features of mature neural cells.

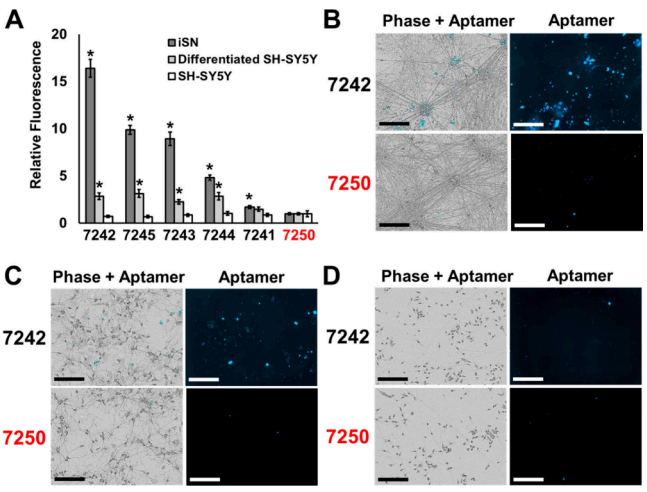

Figure 2. Characterization of DNA aptamers targeting iSNs. (A) Quantification of aptamer and negative control oligonucleotide binding to iSNs, differentiated SH-SY5Y cells, and immature undifferentiated SH-SY5Y cells. Statistical analysis was performed vs negative control 7250 in each cell culture type; $*p < 0.05$. (B−D) Representative images of aptamer 7242 and negative control 7250 binding to target iSNs (panel B), differentiated SH-SH5Y cells (panel C), and negative selection SH-SY5Y cells (panel D). Oligonucleotides were synthesized with 3′ biotin and visualized by poststaining with fluorescently labeled streptavidin (blue). Images are collected at 20× magnification. Scale bar: 200 μM.

We next applied confocal microscopy to further characterize the iSN binding and confirm observations made using phase contrast imaging at a lower resolution. We found that aptamers exclusively bound to highly compact clusters of cell bodies that stain for β-tubulin III, a marker of mature neurons (Figure 3).[16,17] MitoTracker Red CMXRos was included at the time of aptamer staining in order to ensure that stained cells contained intact, functional mitochondria, a positive indicator of cell health under aptamer binding conditions. Interestingly, although aptamer binding solely overlaps with regions of β-tubulin III staining in MitoTracker-positive cells, candidate aptamers did not bind mature iSN neurites. Negative control 7250 was used in these studies to establish background nonspecific binding of biotinylated oligonucleotides and fluorescent streptavidin.

Aptamers that bound to iSNs but not immature SH-SY5Y cells were then applied to DRGOs as a single-dose treatment to screen for biological effects on neurite outgrowth. DRGOs were generated from fibroblast donor sources used for aptamer selection and prepared under culture conditions promoting neurite outgrowth. Aptamers were added to FBS-free neurite

https://doi.org/10.1021/acschemneuro.5c00162
ACS Chem. Neurosci. 2025, 16, 1258−1263

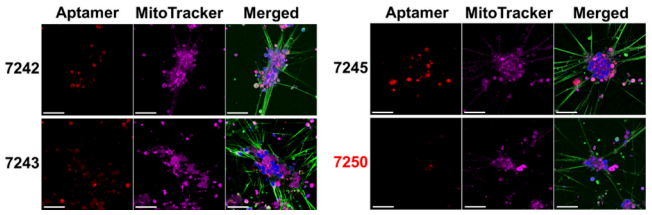

Figure 3. Confocal microscopy demonstrates aptamer binding to iSN cell bodies. Representative images of aptamers 7242, 7243, and 7245 binding to iSN cells co-stained with mature neuron-specific β tubulin III (green) and DAPI (blue). 3′-Biotinylated aptamers were detected by poststaining with fluorescent streptavidin (red). Negative control oligonucleotide 7250 demonstrates minimal background streptavidin staining or nonspecific interactions under binding conditions. Aptamer binding is exclusive to cell bodies and not found on neurites. Images were collected at 40× magnification. Scale bar: 50 μM.

outgrowth media at a final concentration of 1 μM following adherence of DRGOs to the plate surface (day zero). Aptamer-exposed DRGOs were allowed to proliferate for 4 days, at which point neurite outgrowth was measured with blinding and compared to values recorded on day zero. Neurite outgrowth was quantified by tracing of the outer neurite perimeter in micrographs taken at the time of treatment (day zero) and after 4 days of growth (Supplemental Figure S3). Fold change in mean neurite radius, mean neurite area, and mean organoid radius were quantified using CellProfiler software over the course of the assay to measure any effects of aptamer treatment.[18]

Interestingly, aptamers 7242, 7243, and 7245 were found to promote modest neurite outgrowth in a screen of single-concentration, single-dose results compared to nonbinding negative control 7250 (Figure S3). After using this screen to identify a lead aptamer, we treated independently differentiated DRGOs with a series of concentrations of aptamer 7242 to identify an optimal treatment condition (Figure 4). We found that a single treatment of 500 nM aptamer significantly increased neurite area, while higher doses had reduced impact. Notably, the negative control oligonucleotide 7250 reduced neurite outgrowth at the highest dosage applied, suggesting that high concentrations of any oligonucleotide may have unexpected inhibitory effects. The neurite growth effects reported here are statistically significant but moderate and may be improved by further optimization of the treatment conditions. Nonetheless, we note that 7242 is the first aptamer reported to promote neurite extension in models of developing human neurons.

Aptamer 7242 is the most iSN-specific (Figure 1A,B) and biologically active (Figure 4) sequence selected here. We next sought to identify the active cell-binding region of 7242 by systematically generating a series of truncated molecules based on predicted structural elements. mFold was used to construct a predicted two-dimensional structure of 7242.[19] This structure guided the processive elimination of portions of the aptamer until a nonbinding molecule was isolated, indicating that the active region had been removed (Figure S4A,B). We found that nucleotides 8−41 of the 80 nt sequence contain the active iSN binding region of 7242 by demonstrating that other elements could be removed without significant loss of function (Figure S4C). One truncated version, which removed nucleotides 1−8, displayed moderately improved binding versus the original full-length molecule. This may result from

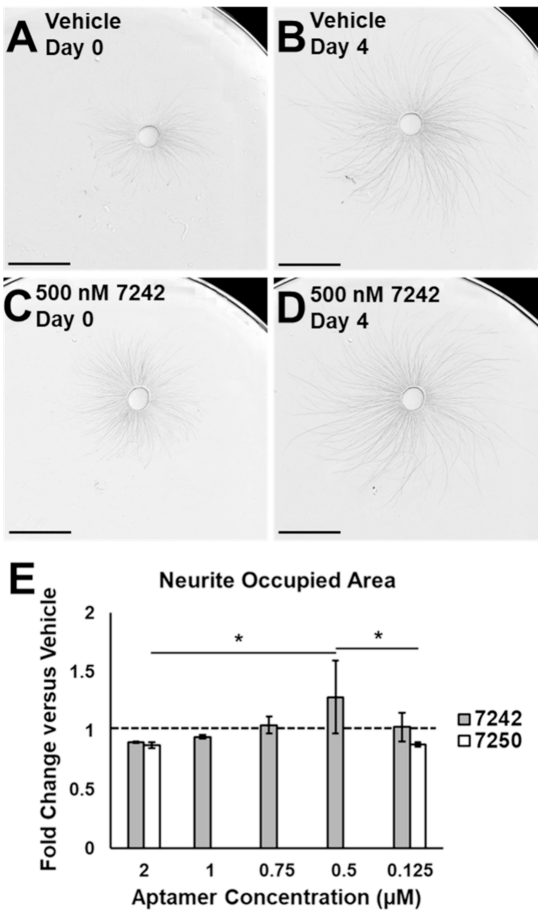

Figure 4. DRGO neurite area is increased by treatment with aptamer 7242. DRGOs are imaged prior to and following 4 days of treatment in culture with a single dose of aptamer 7242, negative control 7245, or vehicle. (A) DRGO prior to treatment with vehicle. (B) DRGO following 4 days of treatment with a single dose of vehicle. (C) DRGO prior to treatment with 500 nM aptamer 7242. (D) DRGO following 4 days of treatment with a single dose of aptamer 7242. (E) Neurite occupied area is quantified by manual tracing of blinded images. Results are measured as fold change in area over the four-day treatment course and normalized to treatment with vehicle. *$p < 0.05$. Scale bar: 3.2 mm.

the elimination of steric interference from these nucleotides, which are immediately neighboring the active region of the aptamer and are predicted to be unstructured (Figure S4B). This effort identifies smaller lead molecules for a future study.

These results suggest that unmodified DNA aptamers can be useful cell-specific reagents to regulate neurite outgrowth. Further analysis, including aptamer target identification, altered RNA expression profiling, and examination of mature neuronal protein abundance, will be required to uncover mechanistic details. Although we selected aptamers capable of binding iSNs derived from multiple healthy donors, this work raises the possibility of developing either patient-specific or disease-specific aptamers that may have relevance in specific targeted contexts. Importantly, the unique properties of nucleic acid selection by evolutionary principles enable the identification of aptamers targeting highly specific cell populations without requiring a known distinctive molecular feature. This is particularly valuable in the context of neuronal diseases, in which nonspecific effects on healthy neurons may be highly deleterious. We envision that cell-specific DNA aptamers could

https://doi.org/10.1021/acschemneuro.5c00162
ACS Chem. Neurosci. 2025, 16, 1258−1263

also have potential application in modifying in vitro cell development or in targeted delivery of molecular cargo to mature neuronal cells. Future studies selecting aptamers targeting iPSCs might likewise identify DNA affinity reagents capable of promoting development toward neural or other cell types.

MATERIALS AND METHODS

Cell Culture. SH-SY5Y cells were cultured in DMEM:F12 (Gibco, 11330057) with 10% FBS (R&D Systems, S11550H) and 1% penicillin−streptomycin (Gibco, 15140122). These cells were maintained at 20% oxygen and 5% CO_2.

Buffers. Wash buffer was DPBS (Gibco, 14190-144) supplemented with 5 mM $MgCl_2$ and 4.5 g/L glucose. Binding buffer was DPBS supplemented with 5 mM $MgCl_2$, 4.5 g/L glucose, 100 μg/mL tRNA, and 100 μg/mL BSA.

Oligonucleotides. DNA libraries, primers, and aptamers were purchased from Integrated DNA Technologies (Coralville, IA) with standard desalting. All sequences and modification abbreviations are provided in Supplemental Table S1.

DNA Aptamer Selection. Fully differentiated (d-d) iSN cells growing on Geltrex-coated 6-well culture dishes served as the target cell line for DNA aptamer selection. SH-SY5Y cells were used as negative selection cells at ∼80% confluency also on Geltrex-coated 6-well plates. Naive DNA libraries were purchased from Integrated DNA Technologies (Coralville, IA) with standard desalting. For round 1, 2 nmol (∼1.2×10^{15} molecules) of random DNA library 6859 was prepared in 4.5 mL of wash buffer, heated at 90 °C for 5 min, and snap cooled on ice. tRNA (100 μg/mL) and BSA (100 μg/mL) were then added as competitors. The following 14 rounds used 200 pmol of large-scale PCR amplified and purified library recovered from each previous round. Media was aspirated from SH-SY5Y cells, and the wells were rinsed once with wash buffer. 2 nmol (round 1) or 200 pmol (rounds 2 and later) of library prepared in 4.5 mL of wash buffer was added to the negative selection cells and incubated for 30 min. Media was then aspirated from iSN cells, and the dish was rinsed once with wash buffer. The library solution was transferred from the SH-SY5Y cells to the washed iSN cells and incubated for another 30 min. Adherent iSN cells were then washed three times with wash buffer at room temperature, scraped into wash buffer, and collected by centrifugation (500 × g for 5 min). The supernatant was removed, and the cell pellet was resuspended in 500 μL of wash buffer. Cells were then lysed, and macromolecules were denatured by heating at 95 °C for 10 min. Debris was removed by centrifugation at 13,100 × g for 5 min, and the supernatant containing the recovered library was transferred to a fresh tube.

For only the first selection round, the recovered cell pellet was resuspended in water and used in its entirety as the template for PCR with the following reagent volumes: 500 μL of round 1 lysate, 100 μL of 10× PCR buffer, 80 μL of 2.5 mM dNTPs, 100 μL of 1 mg/mL BSA, 80 μL of 50 mM $MgCl_2$, 50 μL of forward primer 6638 (10 μM stock), 50 μL of reverse primer 6860 (10 μM stock), 20 μL of water, and 20 μL of Taq DNA polymerase (Invitrogen, 10342178). The mixture was split into 100 μL aliquots and subjected to thermal cycling (94 °C, 60 s; 8 × (94 °C, 30 s; 52 °C, 35 s; 72 °C, 30 s)).

The lysate (or the completed PCR solution in the case of the first round) was used directly as a template for analytical PCR to determine the optimum number of cycles to be used in a large-scale PCR. The following reagent volumes were used: 200 μL of template, 200 μL of 10× PCR buffer, 160 μL of 2.5 mM dNTPs, 200 μL of 1 mg/mL BSA, 160 μL of 50 mM $MgCl_2$, 200 μL of forward primer 6638 (5 μM), 200 μL of reverse primer 6860 (5 μM), 652 μL of water, and 28 μL (140 units) of Taq DNA polymerase. The mixture was split into 100 μL aliquots and subjected to thermal cycling following the protocol described above with the optimum number of cycles as determined with analytical PCR.

Following amplification, aliquots were recombined. 0.1 volume of 3 M NaOAc was added and mixed. Nucleic acids were precipitated by the addition of 2.5 volumes of ethanol, mixing, incubation on dry ice for 15 min, and centrifugation at 17,000 × g for 15 min. The pellet was washed with 70% ethanol followed by centrifugation at 17,000 × g for another 15 min. The pellet was air-dried, resuspended in 40 μL of water, combined with 160 μL of deionized formamide, heated at 90 °C for 5 min, loaded onto a 10% denaturing polyacrylamide gel (7.5 M urea, 19:1 acrylamide/bisacrylamide)), and subjected to electrophoresis for 2 h at 600 V (26.25 V/cm).

Bands were visualized briefly with a hand-held UV lamp. The higher mobility DNA band containing the fluorescent single-stranded library was excised by using a clean razor blade. This material was diced and eluted overnight at 37 °C in 500 μL of 2× PK buffer (100 mM Tris-HCl (pH 7.5), 200 mM NaCl, 2 mM EDTA, 1% SDS) on an end-over-end rotator. The supernatant was extracted with an equal volume of phenol/chloroform/isoamyl alcohol (25:24:1) (VWR, 97064-692). The upper aqueous phase was then precipitated from ethanol, as described above. The pellet was resuspended in 100 μL of water. The concentration of the resulting DNA library was estimated using a molar extinction coefficient of 766,275 $L \cdot M^{-1}$ cm^{-1} at 260 nm.

Immunofluorescence Staining and IncuCyte SX5 Imaging. Cells were washed with wash buffer (defined above) to remove debris from the culture before staining. Aptamer solution (200 nM aptamer in wash buffer) was heated at 90 °C for 5 min and snap cooled on ice. Salmon sperm DNA was added to a final concentration of 100 μg/mL to inhibit nonspecific aptamer binding. Aptamer solutions (200 nM in wash buffer) were added to cells for 1 h at 37 °C. Cells were washed three times with wash buffer and incubated with 3.7% formaldehyde for 15 min at room temperature. Cells were washed twice with wash buffer and incubated with streptavidin−Alexa Fluor 647 conjugate (Invitrogen, S21374) secondary stain at 1:500 dilution in DPBS for 1 h at room temperature. Cells were washed three times with DPBS and imaged with IncuCyte SX5 (Sartorius) at 20× magnification. Quantification of aptamer staining was calculated as the total integrated intensity per image field, with 35−47 replicates per condition.

Confocal Imaging. iSNs were prepared as described in the Supporting Information on 35 mm glass-bottom dishes (Mattek, P35G-1.5-14-C). Aptamer solutions (200 nM in wash buffer) were added to cells for 1 h at 37 °C. Cells were washed three times with wash buffer and incubated with 3.7% formaldehyde for 15 min at room temperature. Fixed cells were permeabilized with 0.25% Triton X-100 for 20 min before being washed once and blocked for 2 h in SuperBlock blocking buffer (Thermo, 37580). Cells were then stained overnight at 4 °C with 1:500 Tuj-1 primary antibody (Proteintech, 66375-1-lg) in blocking buffer (SuperBlock including 0.05% Triton X-100). Cells were then washed with PBS and stained with 1:2000 secondary antibody (Invitrogen, A28175) and 1:500 AlexaFluor647−streptavidin (Thermo, S21374) in blocking buffer for 1 h at room temperature. Specimens were then stained with DAPI (Roche, 10236276001) before imaging on an LSM780 confocal microscope.

DRG Organoid Neurite Outgrowth Assay. Differentiation of iPSCs into an organoid model of DRGs (DRGOs) was based on a previously reported approach with modification.[12] iPSCs were dissociated into single cells using Accutase and resuspended in mTeSR supplemented with Y-27632 (5 μM). 9×10^3 cells in 125 μL were plated per well in V-bottom plates (Nunc) followed by centrifugation at 100 × g for 5 min (DIV −2; DIV = days in vitro where day 0 begins differentiation).[12] The following day (DIV −1), 125 μL of KSR media supplemented with β-mercaptoethanol (100 μM) was added to each well. At DIV 0 and DIV 2, approximately half of the media was exchanged for KSR media with β-mercaptoethanol (KSRb), LSB (100 nM LDN193189 and 10 μM SB431542). At DIV 4, the medium was changed to 1 part N2-based media (Neurobasal media supplemented with N-2) and 3 parts KSRb media supplemented with LSB and 3i (3 μM CHIR99021, 10 μM DAPT, and 3 μM SU5402). At DIV 6, the medium was changed to 1 part N2-based media and 1 part KSRb supplemented with LSB and 3i. At DIV 8, the medium was changed to 3 parts N2-based media and 1 part KSRb media supplemented with LSB and 3i. At DIV 10, the medium was changed to neuronal maintenance media (10 ng/mL NGF, 10 ng/mL BDNF, 10 ng/mL GDNF, 10 ng/mL NT3, and 200 μM L-

https://doi.org/10.1021/acschemneuro.5c00162
ACS Chem. Neurosci. 2025, 16, 1258−1263

ascorbic acid in N2-based media). Half of the medium was replaced every 2 to 3 days. DRGOs (DIV 36) were plated into Geltrex-coated 24-well plates, and experiments were initiated 48 h postplating.

For neurite outgrowth assays, DRGOs were treated by the addition of aptamer at indicated concentrations and monitored via Incucyte imaging every 12 h for 4 days without washing or aptamer replenishment. Micrographs of organoids that adhered through this period were analyzed at the initial and end time points using CellProfiler in a blinded fashion. The area occupied by neurites was identified and manually circumscribed along the neurite periphery in each image of multiple organoids at both time points. Metrics were calculated as a ratio of the final time point (day 4) versus the initial time point (day 0), and statistics were calculated compared to negative control 7250 using a *t* test.

■ ASSOCIATED CONTENT

Supporting Information

The Supporting Information is available free of charge at https://pubs.acs.org/doi/10.1021/acschemneuro.5c00162.

Additional experimental details, materials, methods, supplemental figures, and oligonucleotide sequences (PDF)

■ AUTHOR INFORMATION

Corresponding Author

L. James Maher III − *Department of Biochemistry and Molecular Biology, Mayo Clinic College of Medicine and Science, Rochester, Minnesota 55905, United States;* orcid.org/0000-0002-5043-6422; Email: maher@mayo.edu

Authors

Brandon Wilbanks − *Department of Biochemistry and Molecular Biology, Mayo Clinic College of Medicine and Science, Rochester, Minnesota 55905, United States*

Jenelle Rolli − *Department of Biochemistry and Molecular Biology, Mayo Clinic College of Medicine and Science, Rochester, Minnesota 55905, United States*

Keenan Pearson − *Department of Biochemistry and Molecular Biology, Mayo Clinic College of Medicine and Science, Rochester, Minnesota 55905, United States*

Sybil C. L. Hrstka − *Department of Neurology, Mayo Clinic, Rochester, Minnesota 55905, United States*

Ronald F. Hrstka − *Department of Neurology, Mayo Clinic, Rochester, Minnesota 55905, United States*

Arthur E. Warrington − *Department of Neurologic Surgery, Mayo Clinic, Rochester, Minnesota 55905, United States*

Nathan P. Staff − *Department of Neurology, Mayo Clinic, Rochester, Minnesota 55905, United States*

Complete contact information is available at: https://pubs.acs.org/10.1021/acschemneuro.5c00162

Author Contributions

#BW and JR contributed equally. Project conception: LJM, NPS, AEW. Experimental work: JR, BW, KSP, SCLH, RFH. Data Analysis: JR, BW, KSP, SCLH, LJM. Manuscript preparation: BW, JR, LJM.

Notes

The authors declare no competing financial interest.

■ ACKNOWLEDGMENTS

This work was supported by NIH grant R35GM143949 (LJM), DOD grant W81XWH-22-1-0313 (LJM), an NSF graduate fellowship (BW), and by the Mayo Clinic Graduate School of Biomedical Sciences. We acknowledge the Mayo Clinic Genome Analysis Core and Microscopy Core for their contributions.

■ REFERENCES

(1) Sneddon, L. U. Comparative Physiology of Nociception and Pain. *Physiology (Bethesda)* **2018**, *33* (1), 63−73.

(2) Margariti, A. Peripheral Neuropathy May Be a Potential Risk of Cardiovascular Disease in Diabetes Mellitus. *Heart* **2014**, *100* (23), 1823−1824.

(3) Feldman, E. L.; Callaghan, B. C.; Pop-Busui, R.; Zochodne, D. W.; Wright, D. E.; Bennett, D. L.; Bril, V.; Russell, J. W.; Viswanathan, V. Diabetic Neuropathy. *Nat. Rev. Dis Primers* **2019**, *5* (1), 1−18.

(4) Rodríguez, Y.; Vatti, N.; Ramírez-Santana, C.; Chang, C.; Mancera-Páez, O.; Gershwin, M. E.; Anaya, J.-M. Chronic Inflammatory Demyelinating Polyneuropathy as an Autoimmune Disease. *J. Autoimmun* **2019**, *102*, 8−37.

(5) Nam, S. H.; Choi, B.-O. Clinical and Genetic Aspects of Charcot-Marie-Tooth Disease Subtypes. *Precis Future Med.* **2019**, *3* (2), 43−68.

(6) Hrstka, S. C. L.; Ankam, S.; Agac, B.; Klein, J. P.; Moore, R. A.; Narapureddy, B.; Schneider, I.; Hrstka, R. F.; Dasari, S.; Staff, N. P. Proteomic Analysis of Human iPSC-Derived Sensory Neurons Implicates Cell Stress and Microtubule Dynamics Dysfunction in Bortezomib-Induced Peripheral Neurotoxicity. *Exp. Neurol.* **2021**, *335*, 113520.

(7) Xie, W.; Strong, J. A.; Li, H.; Zhang, J.-M. Sympathetic Sprouting near Sensory Neurons after Nerve Injury Occurs Preferentially on Spontaneously Active Cells and Is Reduced by Early Nerve Block. *J. Neurophysiol* **2007**, *97* (1), 492−502.

(8) Hansen, R. B.; Sayilekshmy, M.; Sørensen, M. S.; Jørgensen, A. H.; Kanneworff, I. B.; Bengtsson, E. K. E.; Grum-Schwensen, T. A.; Petersen, M. M.; Ejersted, C.; Andersen, T. L.; Andreasen, C. M.; Heegaard, A.-M. Neuronal Sprouting and Reorganization in Bone Tissue Infiltrated by Human Breast Cancer Cells. *Front Pain Res. (Lausanne)* **2022**, *3*, 887747.

(9) Geisler, S. Vincristine- and Bortezomib-Induced Neuropathies−from Bedside to Bench and Back. *Exp. Neurol.* **2021**, *336*, 113519.

(10) Wright, B. R.; Warrington, A. E.; Edberg, D. E.; Rodriguez, M. Cellular Mechanisms of Central Nervous System Repair by Natural Autoreactive Monoclonal Antibodies. *Archives of Neurology* **2009**, *66* (12), 1456−1459.

(11) Warrington, A. E.; Bieber, A. J.; Van Keulen, V.; Ciric, B.; Pease, L. R.; Rodriguez, M. Neuron-Binding Human Monoclonal Antibodies Support Central Nervous System Neurite Extension. *J. Neuropathol Exp Neurol* **2004**, *63* (5), 461−473.

(12) Wang, L.; Bing, T.; Liu, Y.; Zhang, N.; Shen, L.; Liu, Z.; Wang, J.; Shangguan, D. Imaging of Neurite Network with an Anti-L1CAM Aptamer Generated by Neurite-SELEX. *J. Am. Chem. Soc.* **2018**, *140*, 18066−18073.

(13) Wang, Y.; Khaing, N. L.; Li, N.; Hall, B.; Schmidt, C. E.; Ellington, A. D. Aptamer Antagonists of Myelin-Derived Inhibitors Promote Axon Growth. *PLoS One* **2010**, *5* (3), No. e9726.

(14) Mazzara, P. G.; Muggeo, S.; Luoni, M.; Massimino, L.; Zaghi, M.; Valverde, P. T.-T.; Brusco, S.; Marzi, M. J.; Palma, C.; Colasante, G.; Iannielli, A.; Paulis, M.; Cordiglieri, C.; Giannelli, S. G.; Podini, P.; Gellera, C.; Taroni, F.; Nicassio, F.; Rasponi, M.; Broccoli, V. Frataxin Gene Editing Rescues Friedreich's Ataxia Pathology in Dorsal Root Ganglia Organoid-Derived Sensory Neurons. *Nat. Commun.* **2020**, *11* (1), 4178.

(15) Kovalevich, J.; Langford, D. Considerations for the Use of SH-SY5Y Neuroblastoma Cells in Neurobiology. *Methods Mol. Biol.* **2013**, *1078*, 9−21.

(16) Jiang, Y. Q.; Oblinger, M. M. Differential Regulation of Beta III and Other Tubulin Genes during Peripheral and Central Neuron Development. *J. Cell Sci.* **1992**, *103*, 643−651.

(17) Ferreira, A.; Caceres, A. Expression of the Class III Beta-Tubulin Isotype in Developing Neurons in Culture. *J. Neurosci Res.* **1992**, *32* (4), 516−529.
(18) Carpenter, A. E.; Jones, T. R.; Lamprecht, M. R.; Clarke, C.; Kang, I. H.; Friman, O.; Guertin, D. A.; Chang, J. H.; Lindquist, R. A.; Moffat, J.; Golland, P.; Sabatini, D. M. CellProfiler: Image Analysis Software for Identifying and Quantifying Cell Phenotypes. *Genome Biology* **2006**, *7* (10), R100.
(19) Zuker, M. Mfold Web Server for Nucleic Acid Folding and Hybridization Prediction. *Nucleic Acid Res.* **2003**, *31* (13), 3406−3415.

https://doi.org/10.1021/acschemneuro.5c00162
ACS Chem. Neurosci. 2025, 16, 1258−1263